Engineering Structures ▮ (▮▮▮▮) ▮▮▮–▮▮▮

Contents lists available at ScienceDirect

Engineering Structures

journal homepage: www.elsevier.com/locate/engstruct

Nonlinear F.E. analysis of Montreal Olympic Stadium roof under natural loading conditions

Massimiliano Lazzari [a], Massimo Majowiecki [b], Renato V. Vitaliani [a], Anna V. Saetta [b,*]

[a] University of Padova, Department of Construction and Transportation, via Marzolo 9, Padova 35131, Italy
[b] University IUAV of Venezia, Department of Architectural Construction, Dorsoduro 2206 - Venezia, 30123, Italy

ARTICLE INFO

Article history:
Received 27 August 2007
Received in revised form
26 May 2008
Accepted 2 July 2008
Available online xxxx

Keywords:
Montreal Stadium roof
Wind action
Cable-suspended structures
Geometrical non-linearity
Finite elements
Time-domain approach

ABSTRACT

The roof over the Montreal Stadium is composed of a pre-tensioned membrane combined with an eccentric cable-stayed system, i.e. the structure is non-symmetric, which leads to a non-uniform structural response under variable static loads. The Montreal Stadium roof is modelled by finite element method as a three-dimensional structure, accounting for geometrically non linear behaviour.

The paper begins by analyzing the free vibrations of the structure, then goes on to consider the static as well as the dynamic effects of wind and snow. The loads induced by wind are simulated as deformation-dependent forces, i.e. follower loads. These analyses enable the structural mechanisms that caused the failure of the roof membrane to be described and better understood. In particular, the paper deals with the first failure, which occurred in an apparently unexceptional condition of wind velocity.

1. Introduction

Nowadays, civil structures become more and more wind and snow sensitive, because of the trend towards lightweight construction and the evaluation of exact wind loads acting on such structures, frequently characterized by complex geometries, requiring expensive experiments in wind tunnels or semi-empirical methods. The dynamic nature of wind action can cause oscillations and deformations, which can compromise the performance of the roof and, in the worst cases, its structural stability. On the other hand, the static effect of snow represents a dominant load for this type of structure, even reaching as high as 70%–80% of the total load. In [1] Melchers demonstrated that one of the primary causes of collapse (corresponding to approximately 45% of the cases analyzed) lies in an erroneous evaluation of the loading conditions and of the structural response. A number of studies and analyses have been carried out on structures that have completely or partially collapsed:

- due to snow, e.g. the Hartford Coliseum (1978), the Pontiac Stadium (1982), the Milan Sports Hall (1985) and the Montreal Olympic Stadium (1992);
- due to wind, e.g. the Montreal Olympic Stadium (1988);
- due to the effects of snow and water ponding, e.g. the Minnesota Metrodome (1983) inflatable roof.

from the observation of such collapse events, significant information has been collected, and design specifications have been obtained for verification of these structures in ultimate and serviceability limit states. In particular, the great difficulties in assessing and simulating real load conditions have emerged and some considerations about such problems are described, for example in [2–4].

The paper deals with numerical analyses of a significant case study represented by the roof over the Olympic Stadium in Montreal, Canada, which proves to be very vulnerable to snow and wind loading. Actually, one of the main aims of the present study was to contribute towards explaining the failure phenomenon due to wind action that has occurred in the roof of the Olympic Stadium in apparently unexceptional conditions (Fig. 1). Such a failure took place in the presence of a wind of low intensity (approximately 19 m/s) coming to bear at an angle corresponding to approximately 60° between the direction of the wind and the main axis of the roof. Moreover, the structure was characterized prior to failure by an antisymmetric dynamic movement with respect to its lesser dimension inducing an oscillation with amplitude of around 5 m.

Starting from data on geometry, materials, and design details, a new refined numerical model of the structure has been developed and non-linear static as well as dynamic analyses have been carried out. Some considerations on the results obtained by the analyses have been performed with the aim of understanding the complex behaviour of such a structure, showing the mandatory requirement of using non linear analysis.

* Corresponding author. Tel.: +39 0498275622; fax: +39 0498275604.
E-mail address: saetta@iuav.it (A.V. Saetta).

0141-0296/$ – see front matter © 2008 Elsevier Ltd. All rights reserved.
doi:10.1016/j.engstruct.2008.07.010

Fig. 1. Membrane failure between the suspension cones.

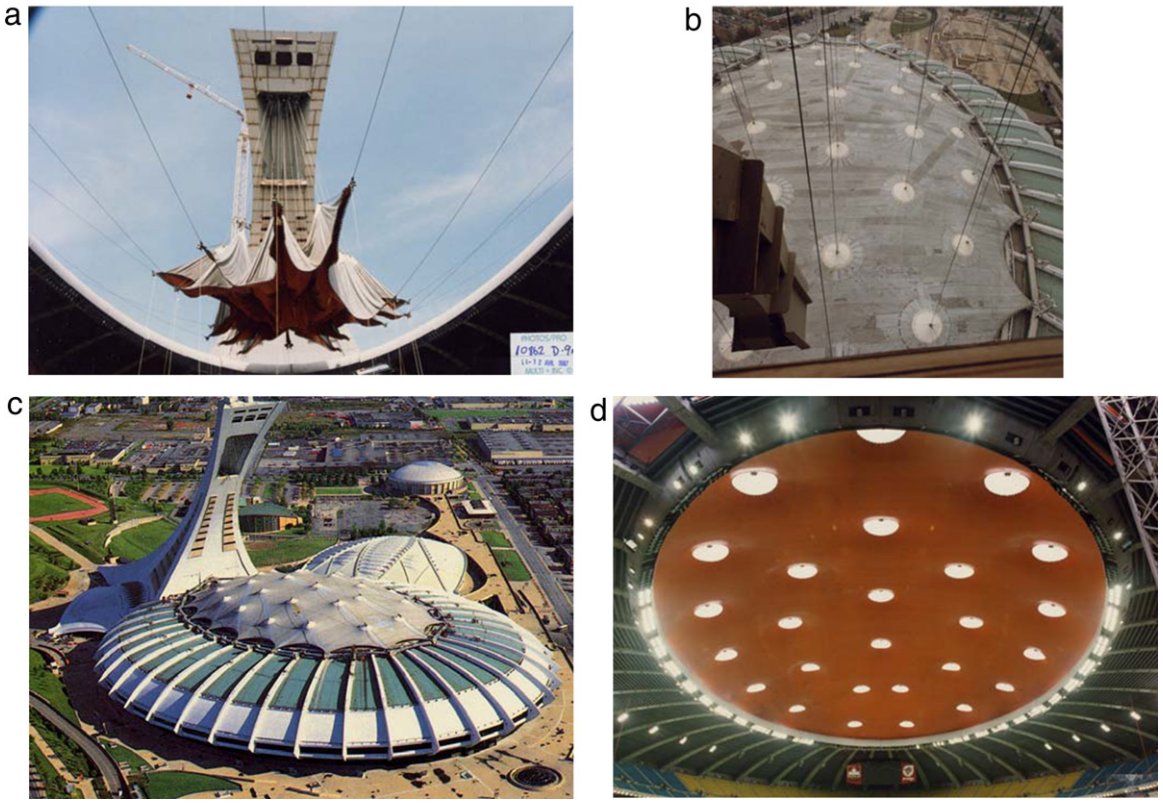

Fig. 2. Membrane motions during the opening phase (a), suspension system (suspension cables, connection cables, perimeter cables and membrane) (b), outside and inside of the roof (c) and (d).

2. The structure

The roof over the baseball stadium in Montreal is a lightweight structure of the cable-stayed system type, with a membrane having a double curvature that covers an ellipse-shaped opening 200 m long and 140 m wide (Fig. 2). The shape of the membrane, i.e. a hyperbolic curvature, was obtained by means of a uniform elliptic pretension, with seventeen points of anchorage around the perimeter and twenty six internal points of suspension as geometric boundary conditions.

The anchorages lie on a steel ring with a hollow rectangular cross-section, whose function is to support the circumferential compression stresses resulting from the geometric-tensional status of the structure; the steel ring is connected to a conventional reinforced concrete roof over the stands. An edge cable ensures the stresses transfer from the membrane to the anchorages.

The twenty six internal supporting points are made with a system of suspension cables hanging from the great inclined tower made of steel and concrete that is the principal roof-supporting structure, as well as the housing system of the roofing structure itself, during periods when it is recovered. The principal cables and the membrane are connected by 40 slender cables departing from the main cable along the directrices of a cone, each ending with a clamp that grips the membrane and, through friction, ensures an almost even distributed transfer of stresses.

Please cite this article in press as: Lazzari M, et al. Nonlinear F.E. analysis of Montreal Olympic Stadium roof under natural loading conditions. Engineering Structures (2008), doi:10.1016/j.engstruct.2008.07.010

Sub-horizontal connection cables are then provided between the internal suspension points and between these and the anchorages on the perimeter ring: such connection cables lie approximately along the horizontal projection of the suspension cables, in other words they lie on a surface including the internal suspension points and the perimeter ring. Their main function is to support the horizontal component of the principal cables forces, enabling the membrane to assume a suitable shape and adequate pretension levels.

The principal characteristics of materials are:

Membrane: The membrane is a "Panama" fabric of Kevlar 49 aramidic fibers, 1420 den, coated with PVC type "B 1086" (Verseidag Industrietextilien, Krefeld, Germany), which guarantees a strength of 490 kN/m in the direction of both the warp and the weave.

The actual tested values show a much higher strength, around 620–640 kN/m in the direction of the warp and 580 kN/m in the direction of the weave. The elasticity modulus is $E = 16$ MN/m, in conditions of biaxial stresses and assuming an average stress range. It is worth noting that the elasticity modulus of membrane element can be given both in the usual unit of measure, that is force per unit of surface (e.g. MN/m^2), and in term of modulus of elasticity per unit length, (e.g. MN/m). This second option is usually adopted by the manufacturers, and is based on the hypothesis that the elasticity modulus represents the stiffness of the membrane element with a definite thickness and not the stiffness of the constitutive material. In this case, the stresses and the strength of membrane also have to be given in such a unit of measure.

To increase the durability of such mechanical characteristics with respect to deterioration due to environmental actions, the PVC protective coating was subsequently further coated with a layer of polyurethane that was coloured according to the recommendations of the membrane's manufacturer: the final thickness was 2.5 mm and the self weight 29 N/m^2. The edges of the membrane were finished off by adopting aluminium shapes and pairs of steel clamps designed to exert a pinching action on the fabric, thus avoiding the need to use punched connections.

Cables: Galvanized harmonic steel strands with an open or closed Z-shaped cross-section were used for the supporting cables of the structure. The minimum ultimate strength was 1.6 kN/mm^2, while the equivalent modulus of elasticity was $E = 1.6E^5$ N/mm^2.

3. The numerical model

The numerical model of the structure: The finite element model of the structure (Fig. 3) uses two types of element: four-node membrane elements and two-node cable elements. The characteristics of each of the finite elements implemented in the "Loki" code are exhaustively described in [3–5]. The overall dimensions of the model amounted to 2452 nodal points for 7356 degrees of freedom, on which 868 cable elements and 1937 membrane elements were built. The main suspension cables and the connection cables were modelled using 4 cable elements; the cables inserted between the membrane and the suspension and connection cables were described by single cable elements, while the perimeter cables were represented by a number of cables varying between 7 and 9. There were 43 points of restraint amounting to a total restraint of 129 degrees of freedom, while the modelling of the mechanical and material characteristics of the structural components was carried out using 12 numerical sets for the cables and just one set for the membrane. For the proposed analysis a linear elastic material model is assumed. A possible further development of such analyses could be the use of non-linear constitutive laws, e.g. [6,7].

Numerical model of the loads: Conservative surface loads have been adopted for simulation of the action of snow, while follower loads description have been adopted for a realistic representation of wind action [8–11]. In fact such an assumption is necessary to describe the load due to wind because of the considerable displacements that occur in the roofing membrane under such varying loads, both in static and dynamic conditions. The self weight of the membrane was 29 N/m^2, the average pretension in both directions was 10 kN/m, the average load due to snow was 1.65 kN/m^2 and the average load due to wind was 0.70 kN/m^2.

4. Static analyses

4.1. '0 state'

The original design idea involved all 26 cables in the operations for lifting and transferring the pretension forces to the roof. Later on, however, these operations were separated with a view to achieving a greater structural simplicity, so 12 cables were used to transfer the pretension action and the other 14 acted for lifting the membrane. The search for the 0 state was done using the same structural model as the one employed for the analyses under static and dynamic external loads (wind and snow). Given the geometric non-linearity of the problem, the procedure is iterative and the initial configuration of every step is assumed equal to the final configuration obtained from the previous iteration.

The mean level of pretension, set in the design phase for the membrane roof, was 10 kN/m. The numerical analyses carried out with the "Loki" code for reproducing the "0" state, give a mean value of stress of about 9.9 kN/m (Fig. 4), in good agreement with the imposed condition.

The peaks of stress, evidenced in the stress contours of Fig. 4, are much localized and they are mainly due to the coarse discretization assumed for the roof, as well as to the distortion of some finite elements of the mesh. Moreover such higher peaks of stress are concentrated in the part of the membrane between the cones.

Finally Table 1 summarizes a comparison between the stress levels on some cables (the first five suspension, connection and perimetrical cables) in the "0" state, obtained with a model of the structure proposed in literature and commented in [5], and by the numerical model of the present study (developed using the "Loki" code). The literature model was made by a network of cables, and the corresponding cable stresses are indicated by σ_{NET}.

It is worth noting that the differences between the numerical results obtained by the "Loki" code analyses and the reference data are minimal for both the main suspension cables and the connection cables, while for the perimetrical cables there are differences at most of about 24%. Such a difference could be ascribed to the fact that such secondary cables usually have a small stress state, especially if compared with the stresses affecting the suspension cables. Therefore, even a negligible variation in the stress state of suspension cables may induce an appreciable variation in the perimeter cables. For this reason, and also due to the minor importance of such secondary cables in the global state of the roof, the observed variations are considered acceptable.

Therefore we can consider the numerical "0" state configuration substantially equivalent to the reference one, so allowing to be used as a suitable basis for the following static and dynamic analyses to be performed on the roof structure.

4.2. Eigenvalue analysis

Starting from the equilibrium configuration obtained by the pretension load condition and by gravitational loads, the eigenvalues and the corresponding eigenvectors have been calculated, arranged in order of increasing frequency; the first 350 were considered, classifying them in three categories:

Please cite this article in press as: Lazzari M, et al. Nonlinear F.E. analysis of Montreal Olympic Stadium roof under natural loading conditions. Engineering Structures (2008), doi:10.1016/j.engstruct.2008.07.010

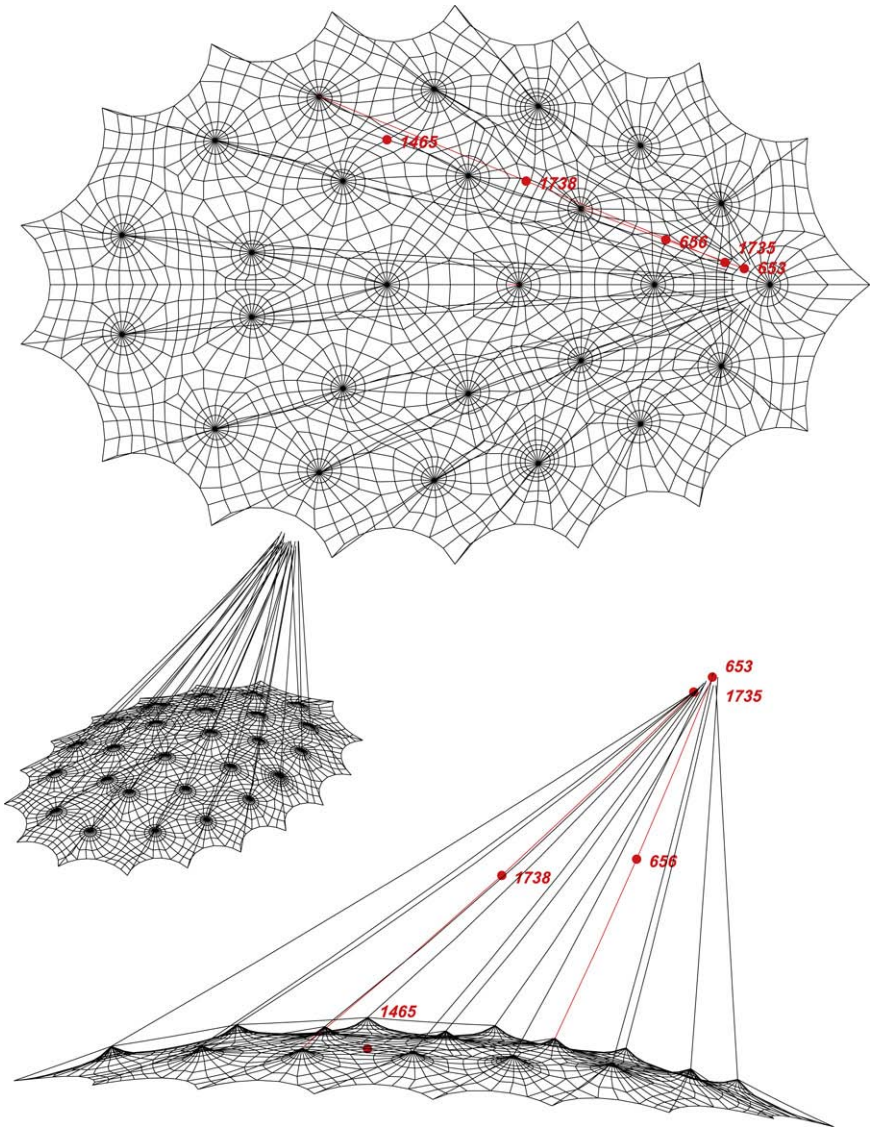

Fig. 3. Finite element model of the roof over the Olympic Stadium in Montreal.

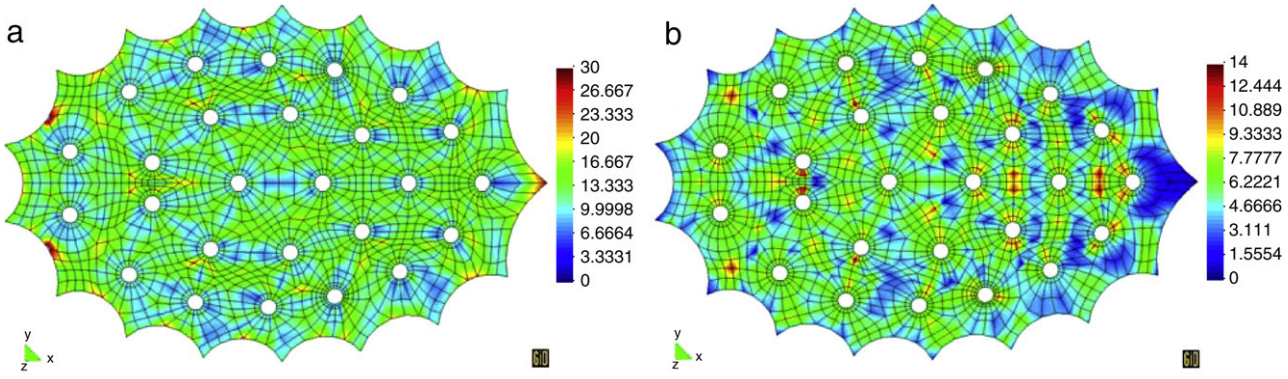

Fig. 4. 1st principal stress (a) and 2nd principal stress (b).

- the first category includes the vibration modes that almost exclusively affect the cables;
- the second category includes the modes in which the vibration of the cables is associated with a relevant vibration of the membrane too;
- the third category includes eigenvectors that mainly affect the membrane, for which the displacement of the cables is almost negligible.

This distinction is also suggested by the distribution of the eigenvectors of these three categories on the frequency field. Fig. 5 shows the shapes of a few eigenvectors with their respective eigenvalues with the aim of describing the

Please cite this article in press as: Lazzari M, et al. Nonlinear F.E. analysis of Montreal Olympic Stadium roof under natural loading conditions. Engineering Structures (2008), doi:10.1016/j.engstruct.2008.07.010

Table 1
Comparison between the cable net equivalent model and the Loki numerical analysis

	Cable	Element	Cross section (mm^2)	σ_{LOKI} (N/mm^2)	σ_{NET} (N/mm^2)	Difference (%)
Suspension cables	1	765–766	5219	225.3	226.3	−0.4
	2	773–774	5219	67.4	65.8	2.4
	3	781–782	5219	139.6	141.7	−1.5
	4	853	4163	49.1	50.6	−2.9
	5	789–790	4163	54.7	57.1	−4.2
Connection cables	1	653–654	5750	267.8	271.3	−1.3
	2	661–662	2875	145.3	146.5	−0.8
	3	669–670	731	147.1	147.6	−0.3
	4	760	731	87.7	85.4	2.6
	5	677–678	4188	211.1	211.3	−0.1
Perimetrical cables	1	537–538	2875	47.5	62.4	−23.9
	2	521–522	2875	79.8	84.5	−5.6
	3	589–590	2875	62.6	80.2	−21.9
	4	523–524	2875	53.5	62.3	−14.1
	5	577–578	2875	60.9	57.0	6.8

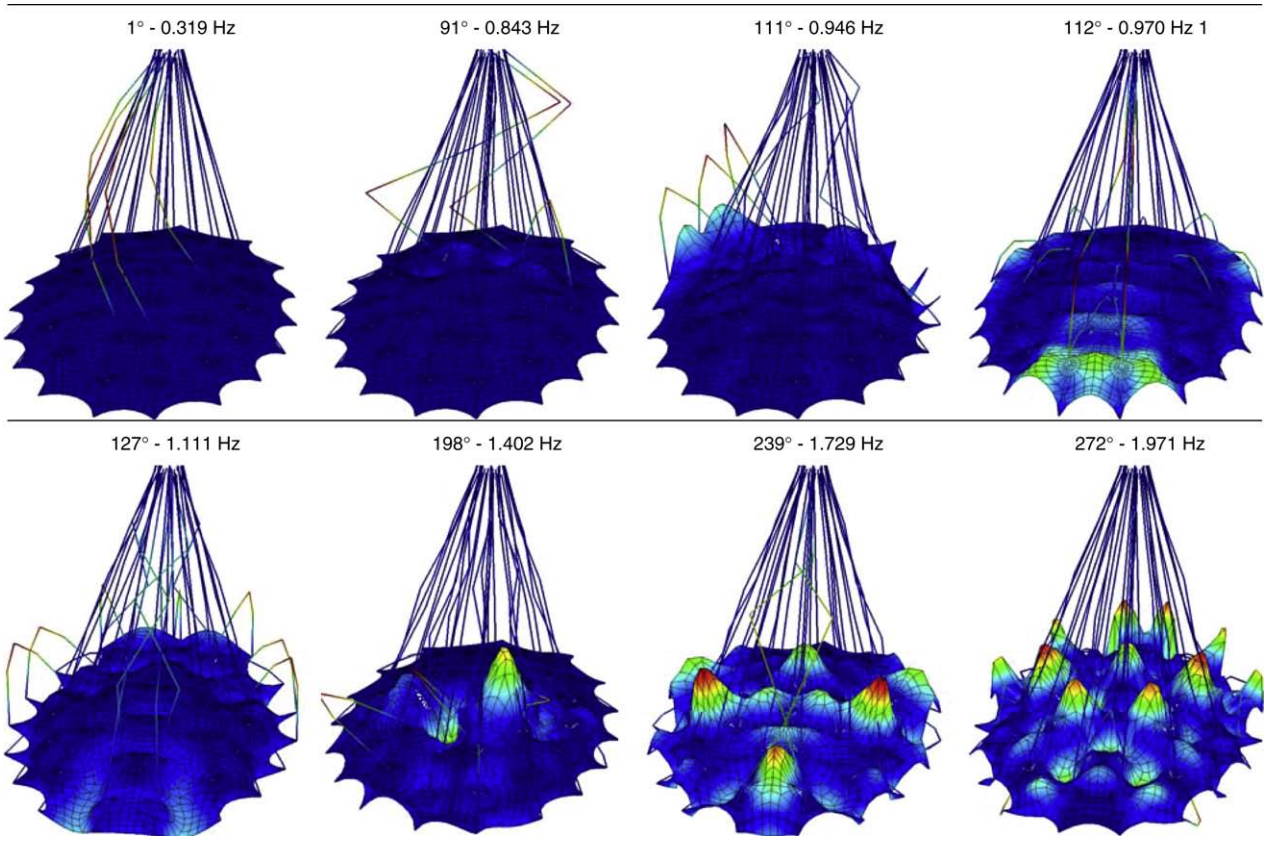

Fig. 5. Eigenvectors and eigenvalues of vibration modes 1–272.

evolution of the vibration modes with increasing frequencies. It is worth noting that the eigenvectors of each category concentrate around specified frequency values, depending on the fundamental harmonic: a first, lower range of frequencies (roughly the first 30) is dominated by vibration modes that fit into the first category; thereafter, vibration modes of the second and subsequently of the third category appear, and their presence becomes progressively stronger.

The results obtained by such an eigenvalue analysis show that not one of the fundamental harmonics involves the entire structure; only with the higher harmonics we can see a global vibration mode. The first eigenvectors are mainly of local type, in limited areas, separated from other parts of the roof structure that remain substantially undisturbed.

Such behaviour is characteristic of the structural roof system: the principal cables, which suspend the roof membrane, prevent the simultaneous movement of all parts of the membrane. Therefore when the lower parts of the cables are in movement, the fundamental modes develop into local modes involving only the membrane near the cones. On the contrary when the lower parts of the cables remain undisturbed, we obtain the higher harmonics that involve the whole structure.

Moreover the exclusive presence of potential vibration modes dominated by the sum of vibrations in limited portions of the roof indicates the small stiffness, or the inadequacy of the pretension, of the structure. The analysis of the eigenmodes of vibration under loading conditions (snow and wind) reveals how the global stiffness characteristics change considerably.

Please cite this article in press as: Lazzari M, et al. Nonlinear F.E. analysis of Montreal Olympic Stadium roof under natural loading conditions. Engineering Structures (2008), doi:10.1016/j.engstruct.2008.07.010

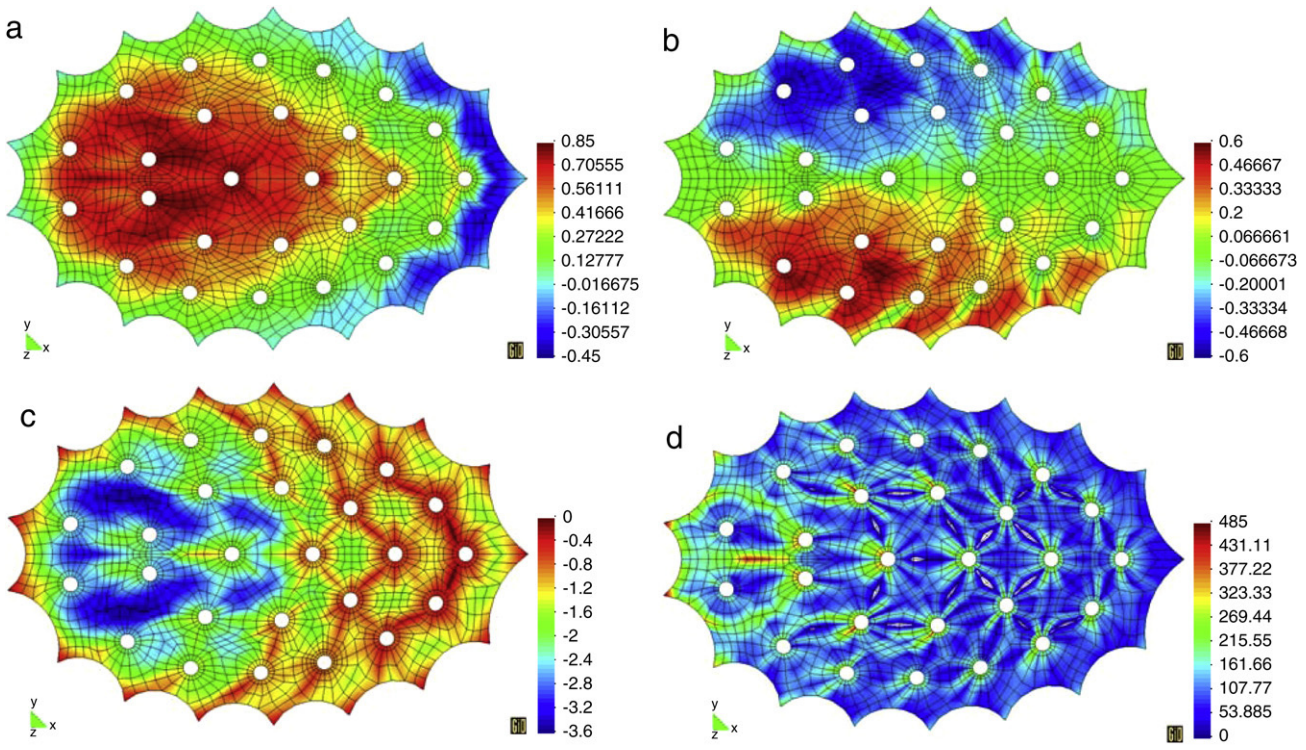

Fig. 6. Snow—displacements [m] X (a), Y (b), Z (c) and 1st principal stresses (d).

4.3. Non linear static analysis with snow and wind

Non linear static analyses have been carried out in "*quasi-static*" conditions, dividing the total load into 100 parts, which have been applied cumulatively at intervals with a step $\Delta t = 1$ s.

Generally speaking, the structure showed a different behaviour between the front (the southern side) and the back (northern side), especially as concerns the displacements. In the next sections the results of the numerical analyses carried out for both load conditions snow and wind, have been summarised and described for each structural element, i.e. membrane and cables.

4.3.1. Snow: Membrane

The displacements calculated on the membrane due to snow load condition are depicted in Fig. 6a, b and c, respectively in the horizontal X and Y directions and in vertical Z direction. The maximum vertical deflection reaches 3.60 m at the front, whereas it does not exceed 2.00 m at the back. Such a difference in the vertical displacements of the roof membrane should not be ascribed to its own deformability, which would lead to a more uniform response (slight variability could be due to differences in the span between the various suspension cones), but rather to the variability of the displacement of the lower ends of the suspension cables.

Actually, such a displacement variability leads to the formation, in some areas of the membrane roof, of "pocket-shape deformations" that facilitate the formation of local snow drifts, in particular in the front (i.e. the southern side) of the roof.

The 1st principal stress (Fig. 6d) exceeds 480 kN/m in the areas where the cables of the cones grip the membrane (i.e. in the radial direction), while it does not exceed 250 kN/m elsewhere. Therefore towards the cones there is the expected concentration of stresses.

As the load increases, the 2nd principal stress diminishes over almost all of the membrane due to the formation of wrinkles which lay down the initial pretension in a circumferential direction around the cones. Such a phenomenon already becomes apparent at 5% of the final load, for which wide areas are no longer stressed, i.e. have lost all their initial pretension. This behaviour emphasizes the inadequate structural stiffness of the roof under the snow loads assumed in the design phase. This low structural stiffness derives from the small value of the contracurvature with respect to the principal dimensions of the membrane panels within the suspension cones. In addition, the membrane suffers excessively from the slanting angle and the length of the suspension cables, showing a markedly different behaviour at the front by comparison with the back.

4.3.2. Wind: Membrane

Unlike the loads due to snow, the effect of wind action causes a part of the roof (to the north) to show a pneumatic behaviour, i.e. the principal cables are unable to work under negative pressure beyond a specific value and the displacement contour shows a "global inflatable effect" (Fig. 7a, b and c) that means that the structure inflates according to a uniform shape (i.e. a membrane behaviour of the structure can be observed), and therefore the different behaviour of the frontal zone with respect to the back one is not very evident, different from the case of snow load.

The point of maximum vertical displacement, of about 1.2 m, is located in the central zone of the membrane, different from the case of snow load for which the maximum deflection is situated in the front area (Fig. 6c); this is due to the fact that the back of the roof no longer has the optimal behaviour that it demonstrated in the case of snow load.

The mapping of the displacements thus shows their tendency to increase radially from the edge towards the middle of the roof and there is no longer any onset of pocket displacements in specific areas. The level of the displacement is determined by the inadequate response of the principal suspension cable system in decompression condition: their contribution to the global stiffness of the structure is soon lost as the load increases.

The 1st principal stress (Fig. 7d) keeps a value of about 140 kN/m in the internal areas between the cones, whereas there is generally

Please cite this article in press as: Lazzari M, et al. Nonlinear F.E. analysis of Montreal Olympic Stadium roof under natural loading conditions. Engineering Structures (2008), doi:10.1016/j.engstruct.2008.07.010

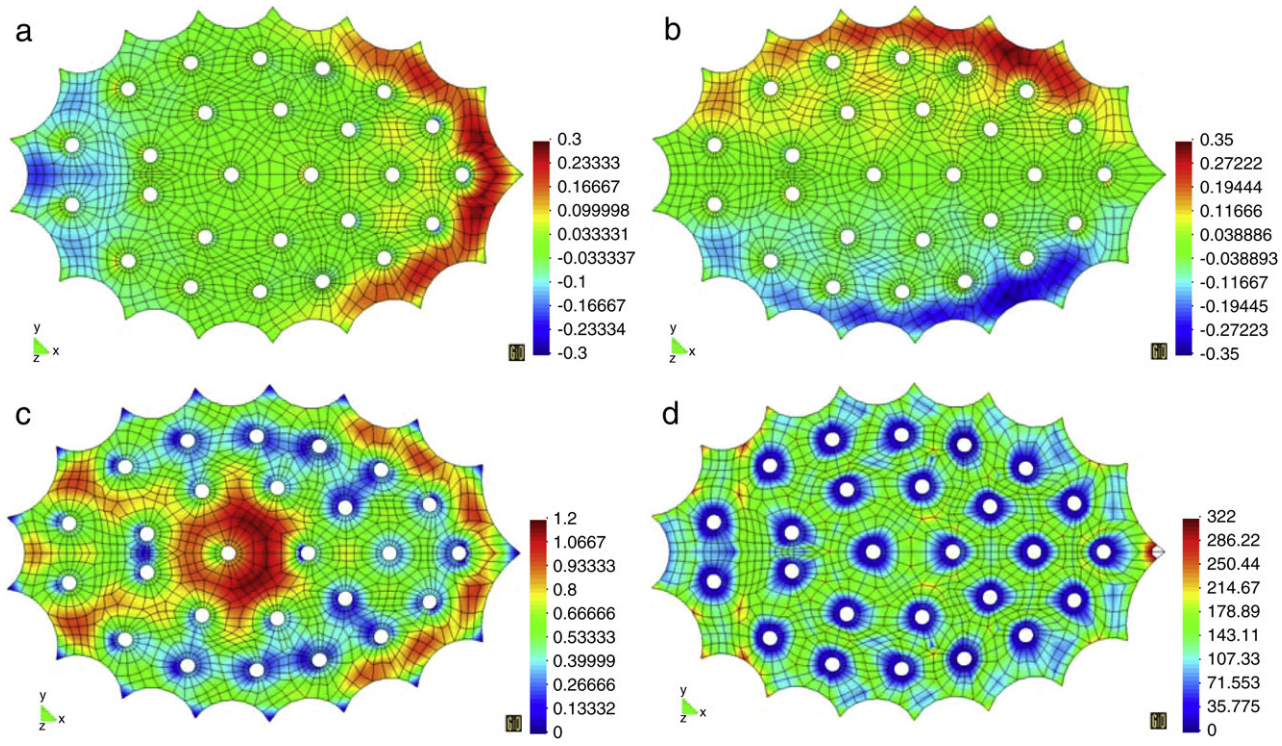

Fig. 7. Wind—displacements [m] *X* (a), *Y* (b) and *Z* (c) and 1st principal stresses (d).

a discontinuity in the stress level around the cones. The 1st principal stress sometimes tapers down to 0, in particular where the cones grip the membrane, where the 1st principal stress is in the circumferential direction. In the radial direction there is a local "throttling" of the membrane due to the tendency of the local curvature to change sign due to the lifting: the stiffening effect attributed to the global curvature fails to contain this tendency and an inversion of local curvature occurs.

Finally Fig. 8 shows displacements and stresses vs load increment for a membrane point for both the wind and the snow cases. In particular, for the snow load, it is clearly evidenced a drastic reduction in the 2nd principal stress in the membrane, which zeroing already for very low load level, while in the case of wind the 2nd principal stress maintains positive but small values. As for the displacement diagrams, for the snow case it is worth noting the presence of a non zero value for all the three components of displacement: the vertical one being the most significant, and the two horizontal ones are symmetrical with respect to zero. On the contrary in the case of wind, only the vertical displacement assumes a significant value.

4.3.3. Snow: Suspension and connection cables

The value and the distribution of the displacements of the principal suspension cables are controlled mainly by their geometry. The cables that support the roof at the front are markedly oblique (about 30°–35° with respect to the horizontal direction) so a vertical downward displacement, which has a significant component in the direction orthogonal to the cable, cannot be easily impeded. Assistance could be given by the sub-horizontal connection cables, which connect the bottom end of two suspension cables between them and to the perimetrical ring. However due to the high inclination between the principal and the sub-horizontal cables (about 160°–165°), the orthogonal resultant force applied to the membrane can hardly oppose to the vertical displacements. The large displacement behaviour that consequently arises is evidenced by the markedly non-linear displacement–load relationship, characteristic of all three displacement components, i.e. Fig. 9a. The displacement–load diagrams are referred to the central points of the cables, while the stress–load diagrams are referred to the upper point jointing each cable with the suspension tower (see Fig. 3). Near the back of the roof, the cables become progressively more vertical, so improving their behaviour under snow load condition. Moreover they are better supported in lateral movements by their respective connection cables and the displacement–load relationship becomes almost linear. The midline deflections of the cables are substantially recovered, and such a recovery mode is non-linear and of asymptotic trend.

Concerning the stress state, it is noticeable that any vertical displacement of the head of the suspension cables at the front does not lead to an increment in the stress state: it simply stretches the cable and reduces the deflection. The state of stress imposed by the pre-stressing is too low and the influence of the geometric response is too strong by comparison with the purely mechanical one. The resulting low tensional state combines with the poor geometrical arrangement of the principal cables with respect to the application of loads due to snow.

The displacement–load diagrams of Fig. 9a evidence a typical behaviour of the oblique cables, that can be summarized in two fundamental phases:

- the first coincides with the geometrical recovery of the deflection at the midline of the cable, characterized by a geometrically distinctly non-linear behaviour;
- the second corresponds to a pseudo-linear displacement–load behaviour.

These two phases confirm that, in the initial stage of loading (up to about 40% of the load), the response is geometrically non-linear, with the onset of major displacements, but subsequently becomes almost linear. The stress in the principal suspension cables increases up to values that always remain below 0.70 kN/mm^2, see Fig. 9a.

Please cite this article in press as: Lazzari M, et al. Nonlinear F.E. analysis of Montreal Olympic Stadium roof under natural loading conditions. Engineering Structures (2008), doi:10.1016/j.engstruct.2008.07.010

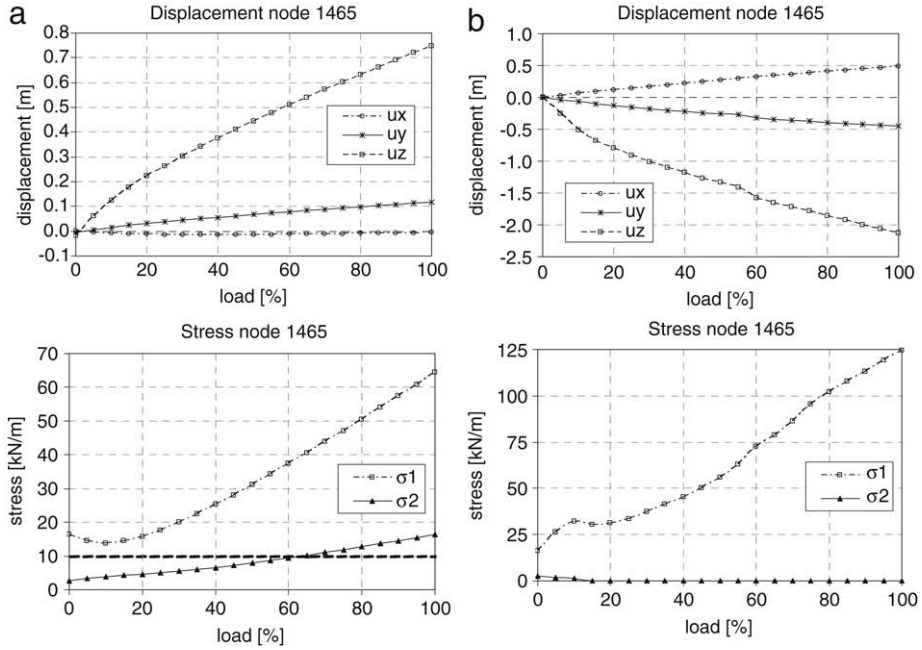

Fig. 8. Membrane displacements and stresses node 1465: (a) snow—(b) wind.

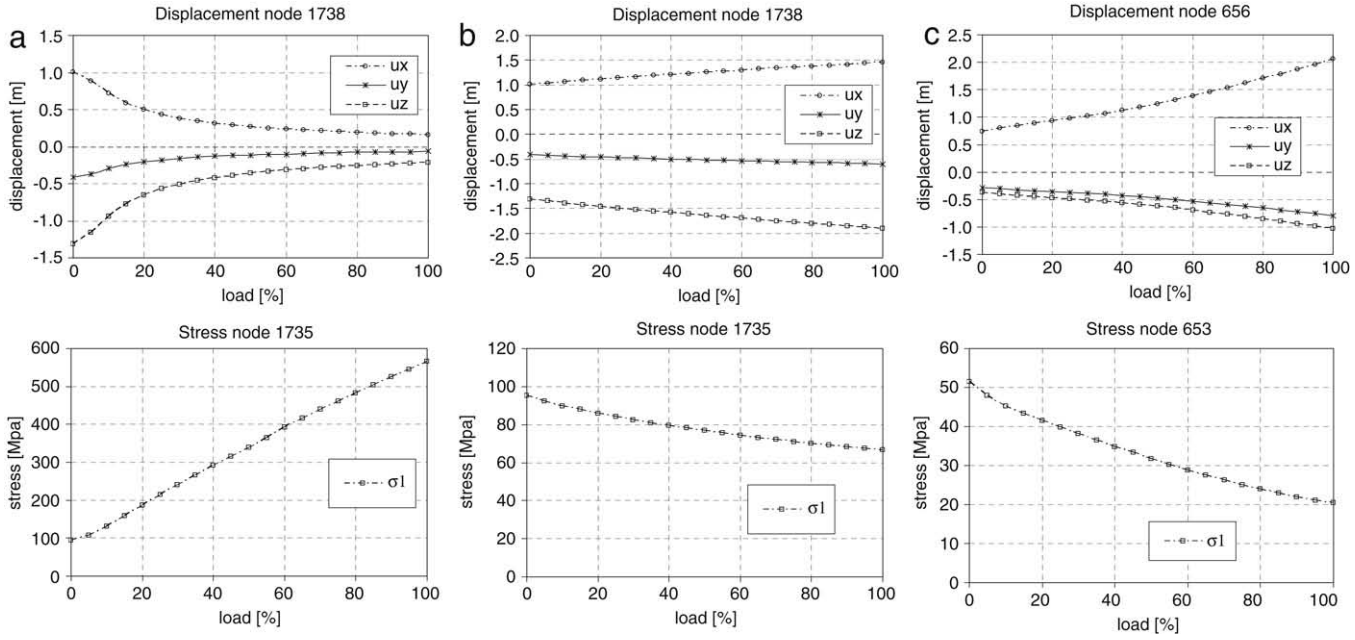

Fig. 9. Suspension cables—displacements and stresses, (a) snow for cable 6 (b) wind for cable 6 (b) wind for cable 10 (c).

In the connection cables, the midline deflections tend to be recovered by the majority of the cables, except for the five at the back and one cable that lies in the median part of the roofing, right on the axis of symmetry. Here again, the stress increases in almost all the cables, reaching a value upper than 0.90 kN/mm^2 in the first cables at the front, while the six previously-mentioned cables tend to be completely unloaded. The trend of the stresses remains strongly non-linear.

The perimeter cable, which works in permanent contact with the membrane, does not undergo any large displacement and it reaches a maximum stress of around 0.80 kN/mm^2 only in three front cables, while in the other cables generally settle around 0.40 kN/mm^2.

4.3.4. Wind: Suspension and connection cables

The geometrical non linear behaviour is evidenced in all the principal suspension cables: both for the frontal, i.e. the more slanting, cables, and the back, i.e. the more vertical cables.

The deflection at the midline of the cables increases consistently, in a *quasi*-linear trend for the slanting cables, e.g. cable 6, Fig. 9b and in a non-linear way for the more vertical ones, e.g. cable 10 Fig. 9c. The load–displacement trend of the cables under wind loading, reveals to be substantially the opposite of what happens under loads due to snow.

Unlike the case of snow load, the back cables behave adequately to lifting up load condition only to less than 50% of the full load. In fact, under the effect of the full load, the pretension applied in the 0 state is almost completely lost.

Please cite this article in press as: Lazzari M, et al. Nonlinear F.E. analysis of Montreal Olympic Stadium roof under natural loading conditions. Engineering Structures (2008), doi:10.1016/j.engstruct.2008.07.010

Already at 60% of the total load, the stress in the principal suspension cables diminishes to values of less than 80 N/mm^2 for the oblique cables (e.g. cable 6) and less than 30 N/mm^2 for the vertical cables (e.g. cable 10).

The loss of tension on the suspension cables releases the membrane from the intermediate supports and the roof, as mentioned earlier, acquires a pressostatic behaviour.

In the connection cables, the midline deflections are recovered to some degree by the majority of the cables, and the stress increases in almost all the cables, reaching a maximum value of about 250 N/mm^2.

Another main difference with respect to loading due to snow concerns the perimeter cable, which also in this load condition does not undergo large displacements, but is subjected to maximum stresses exceeding 500 N/mm^2 along most of its perimeter, and not only at the front, as in the case of snow load.

5. Dynamic analysis: Montreal Olympic Stadium

Due to the flexibility of the roof of the Montreal Olympic Stadium, fluid acts on the directly exposed outer surface of roof as well as on its internal surface depending on the internal volume changes. The roof encloses a fluid volume that can be classified as an appendage of external fluid where the connection is due to exchange surfaces, such as stand access openings, etc. In case of large openings, the fluid field produces point-to-point variable internal pressures, acting on the internal side, which are rather small but not negligible when measured against external pressure level. Conversely, such pressures are not generated when the volume is closed.

The dynamic analysis described in this paper takes into account structure high flexibility and its effects on structural response and applied loads, by introducing the following simplifications:

- structural deformation has no effect on the fluid motion field;
- the constrained fluid volume effect modified by structural movements is introduced with a simplified model for which: (a) structural model speed is small when compared to fluid pressure wave propagation rate; (b) structural periods are high compared with time required for overcoming internal pressure propagation-induced transition.
- wind speed is simulated with a classical Gaussian distribution and speed is transformed into pressure with a quasi-static formula.

In particular, according to the last assumption (that is the basic hypothesis for the wind loading representation), the wind pressure distribution can be obtained starting from the data of the wind velocity field and of the pressure coefficients measured in the wind tunnelling tests. Even if this simplified approach does not account for the real fluid–structure interaction phenomenon, in particular neglects the possible modification of the pressure field due to the structural flexibility, it allows one to capture the main aspects of the global behaviour of such complex non linear structures.

Based on these hypotheses, internal pressure can be considered as distributed quasi-homogeneously and structural dynamics can be described in a simplified form.

The final fluid–structure effect in the foregoing hypotheses is thus given by the algebraic sum of external and internal pressures, both of follower type, due to the structural motion.

These hypotheses allow using the overall macroscopic variables: fluid volume and average internal pressure, both dependent on the environmental conditions, i.e. temperature. Such variables are related by a non-linear law, which has been implemented in the "Loki" Finite Element code, and then solved in the time domain according to the scheme depicted in Fig. 10, which is described in detail in [5]. The interaction scheme between structure and internal

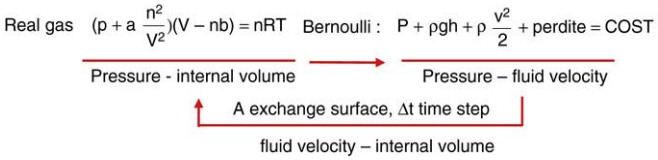

Fig. 10. Interaction model between structure and internal volume.

volume is based on the interactive solution of the real gas relationship, which joints pressure and internal volume, and the Bernoulli laws, which joints pressure and fluid velocity.

The principal variables involved are: gas volume V; gas pressure $p = 101325$ Pa; gas constant $R = 8314$ J/(chilomole K); number of moles n; temperature $T = 298.15$ K (25 °C); a and b constant values related to the considered gas.

The interaction occurs by considering an exchange surface A between outside and inside, which according to the flux velocity can modify the internal volume.

5.1. Test examples

Before proceeding to the direct analysis of the Montreal Olympic Stadium roof structure, the procedure was applied to two simple test examples, particularly suitable to characterize the model's special features. The material parameters and geometrical dimensions of the test examples, Fig. 11, have been chosen such that their features are next to the free oscillation and pretension characteristics recorded in some areas of the Montreal Stadium roof system, with the aim of reproducing a global behaviour similar to that of the Montreal stadium roof itself. Besides the self-weight and the pretension, an external load equal to 240 kN/m^2 for the first three analyses, and equal to 300 kN/m^2 for the fourth analysis, was applied to the structure, orthogonal to the surface, which simulates the mean wind effect which will be assumed in the dynamic analyses of the whole roof structure.

This load was applied statically to the structure, which consequently will found an initial equilibrium configuration. Then such a load has been instantaneously removed and the successive dynamic behaviour of the structure has been studied. Except for self-weight, all the external loads applied to the structure are displacement-dependant follower loads.

The following numerical analyses were completed in this load situation:

- *Analysis* 1: no boundary conditions related to structure–fluid interaction;
- *Analysis* 2: internal volume changes generate opposing internal pressure recalculated at each time step. The number of gas moles in the internal fluid remains unchanged, i.e. outwards fluid exchange is constrained *(impermeable structure or constant volume)*;
- *Analysis* 3: internal volume changes generate opposing internal pressure recalculated at each time step. The number of gas moles in the internal fluid changes, i.e. outwards fluid exchange is enabled, based on exchange surface size *(permeable structure or variable volume)*.
- *Analysis* 4: similar to the previous analysis, with the aim of studying the dynamic of the structure in two consequent time steps.

These analyses were developed to emphasise the response of structures submitted to constant as well as variable volume constraints, with related volume variation versus exchange opening variation. One and two pre-tensioned membrane layer structures were considered, respectively named "one strip" and "two strips" test examples. The membrane structures were characterised, as previously stated, by materials and induced pretensioning as set in the Montreal stadium analysis: in particular the following data have been assumed:

Please cite this article in press as: Lazzari M, et al. Nonlinear F.E. analysis of Montreal Olympic Stadium roof under natural loading conditions. Engineering Structures (2008), doi:10.1016/j.engstruct.2008.07.010

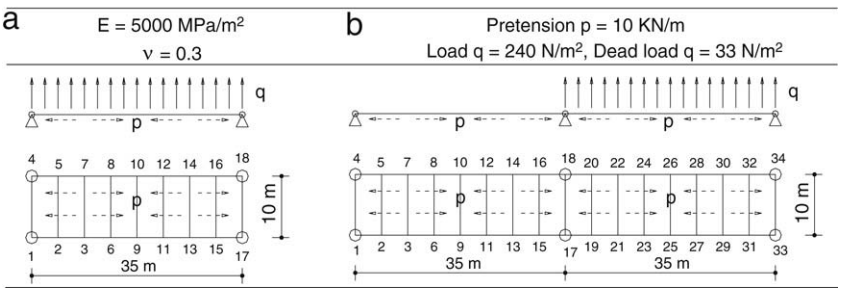

Fig. 11. Geometric dimension and material parameters: 'One Strip Example' (a) and 'Two Strips Example' (b).

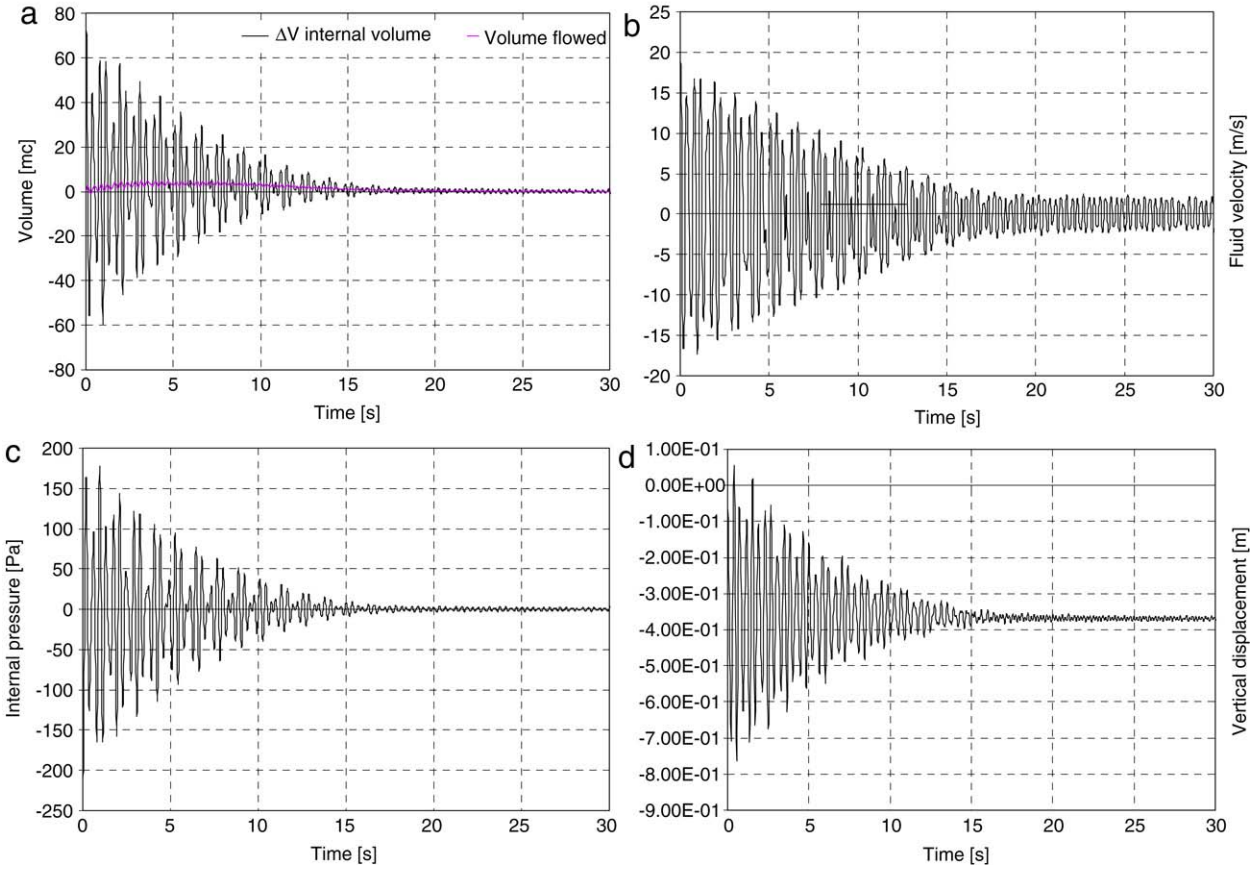

Fig. 12. 'One Strip' — Analysis 3. (a) Internal volume variation, (b) exchange volume and fluid velocity; (c) Internal pressure, (d) vertical displacement Z.

- material parameters: $E = 5000$ MPa/m^2, $\upsilon = 0.3$,
- loading conditions: pretension $p = 10$ kN/m – external load $q = 240$ (300) N/m^2 – dead load $q = 33$ N/m^2.
- the dimensions are assumed to represent a membrane area in the Montreal stadium roof structure front.

5.1.1. One strip example

A 35 × 10 m, elongated rectangular membrane was selected and discretised with 8 finite membrane elements on one line, Fig. 11a. Reference volume, according to Montreal stadium size, was 35 000 m^3. For such a case only the first three analyses were carried out.

As expected the fluid velocity in analysis 2, i.e. impermeable structure, is always zero, as well as the internal pressure in the first analysis, for which no fluid–structure interaction is considered. With reference to analysis 3, Fig. 12 shows the internal volume variation, the exchange volume and the fluid velocity, the internal pressure and the vertical displacement Z. During the first phase of the analysis (between 0 and 15 s) the volume variation due to the structural motion draws an air flux by means of the exchange openings (i.e. the flowed volume). Such a volume decrease as times goes on. In the second phase the flowed volume becomes almost zero and the principal vibration mode of the structure (i.e. the symmetric one) changes to an antisymmetric mode at a higher frequency, for which the volume is preserved. The central point of the strip (nodes 9 and 10, Fig. 11a) remains almost immobile, so evidencing the antisymmetric oscillation, Fig. 12d.

By comparing the three analyses, it is clear that the volumetric bond induces a variation of the vibration modes (towards higher frequency modes) and also introduces an additional damping, particularly for the symmetrical modes, which do not preserve the internal volume (i.e. constant oscillation for the first two analyses and damped oscillation for the third one, see Fig. 12d).

5.1.2. Two strips example

A twice longer 70 × 10 m rectangular membrane was considered, Fig. 11b. The structure was constrained at its 4 corners

Please cite this article in press as: Lazzari M, et al. Nonlinear F.E. analysis of Montreal Olympic Stadium roof under natural loading conditions. Engineering Structures (2008), doi:10.1016/j.engstruct.2008.07.010

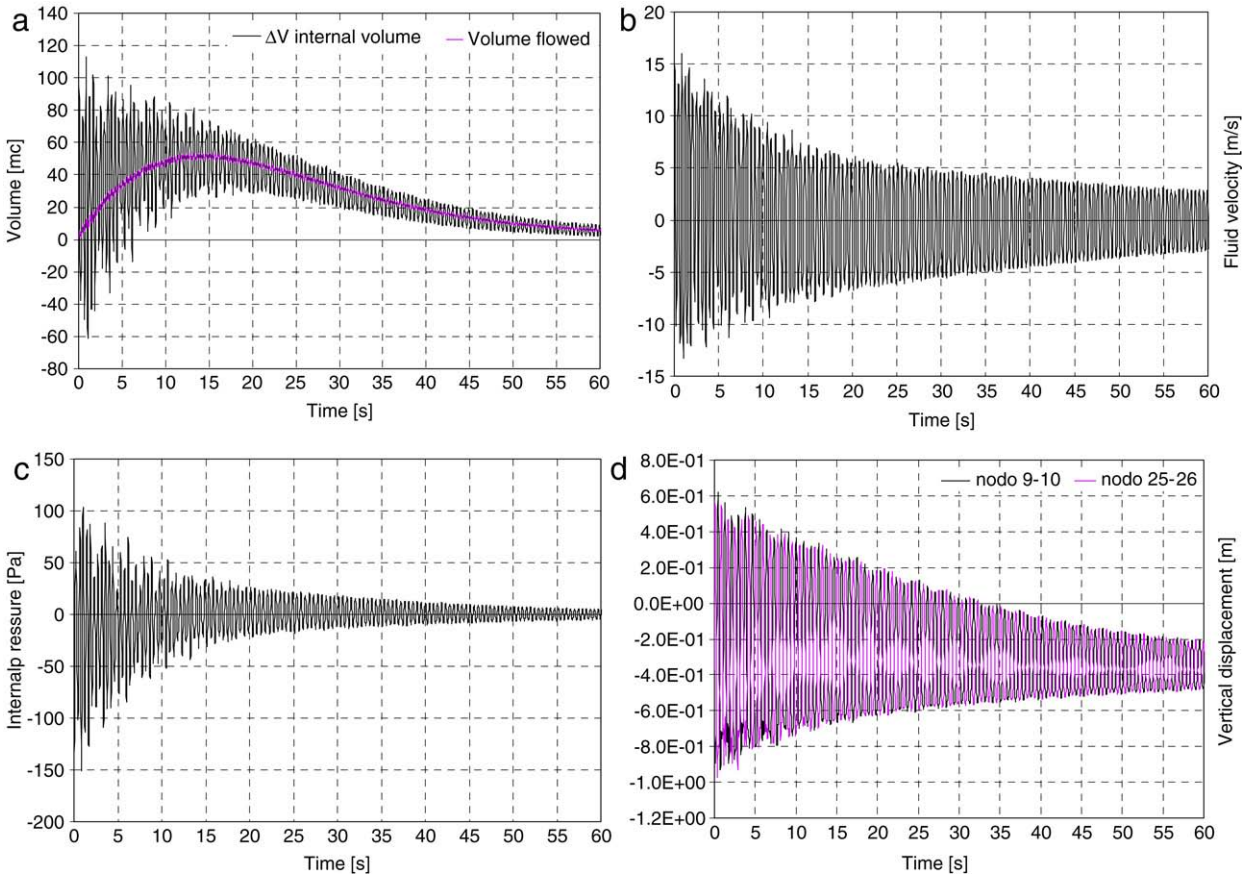

Fig. 13. 'Two Strips' — Analysis 3. (a) Internal volume variation, (b) exchange volume and fluid velocity; (c) Internal pressure, (d) vertical displacement Z.

and at the 2 nodes at the minor symmetry axis. A total of 16 finite membrane elements on one line have been used and the reference volume was 70 000 m^3. Only half the structure has been loaded with the external load q.

The first three analyses show that loads can be transferred from the loaded structural part to the other one, and that the two structurally independent basic strips parts are only constrained together by fluid dynamic laws: they affect each other in the dynamic evolution consequent on external load disappearance.

Similarly to the previous case, Fig. 13 shows the principal results of the third analysis in terms of internal volume variation, exchange volume, fluid velocity, internal pressure and the vertical displacement Z.

All three analyses have been carried out by considering a self weight of 33 N/m^2. Therefore the strips oscillate around a value of about −0.35 m Fig. 13d, differently from the previous analysis, for which the oscillations occurred around zero, Fig. 12d.

For the first analysis no interaction takes place between the left and the right part of the strip, due to the fact that no relationship between structure and internal volume has been considered. In such a hypothesis the solutions for the two strips case are exactly the same obtained for the single strip.

Analysis 3, for the case of two strips, confirms and strengthens the results obtained for the single strip: as time increases, due to the interaction with internal volume, the structure that initially oscillates only on one side, reaches an antisymmetric oscillation which involves the internal volume conservation. Initially the flowed volume (between 0 s and 15 s) increases, and subsequently the flowed volume decreases approaching to zero as the structure starts to oscillate in an antisymmetric way, characterized by constant volume condition.

The purpose of the fourth analysis was to demonstrate internal volume dynamics in two consecutive time intervals (Fig. 14). Half of the structure, namely one of the two basic strips, was submitted to 300 N/m^2 suction load during the first 30 s time span. In such a phase the fluid recall increases the internal volume and external and internal pressures were balanced. Depression state induced inside the structure decreases with time (Fig. 14c—time = 30 s). and internal volume increases due to air entering through the outside opening (Fig. 14a—time = 30 s). The geometrical configuration of both strips at the end of this time step corresponded to static response with no volume constraint (the right part is subjected to a constant pressure of 300 N/m^2 and the left side is subjected only to its self weight equal to 33 N/m^2). In particular, the right hand strip reached maximum size while the left hand one returned to its initial equilibrium configuration.

At the end of the first phase, the external load was removed and the structural part so far loaded started oscillating downwards though contrasted by the internal volume reaction during the second phase of 90 s duration: the internal pressure was higher than the external pressure, with slight oscillations around a gradually changing equilibrium position; the system returned to equilibrium with external pressure and the structure went back to its initial geometrical configuration. The initial structural dynamic of both strips was disordered (Fig. 14c — time = 30–40 s) and later became antisymmetric oscillation (Fig. 14c — time = 60–80 s).

5.2. Results of test examples

It is just noted that simulations have the purpose of underlining the constraint given by the volume subtended to the roof structure and its influence on structural response. In particular, the only possible comparison to check the procedure is with the physical

Please cite this article in press as: Lazzari M, et al. Nonlinear F.E. analysis of Montreal Olympic Stadium roof under natural loading conditions. Engineering Structures (2008), doi:10.1016/j.engstruct.2008.07.010

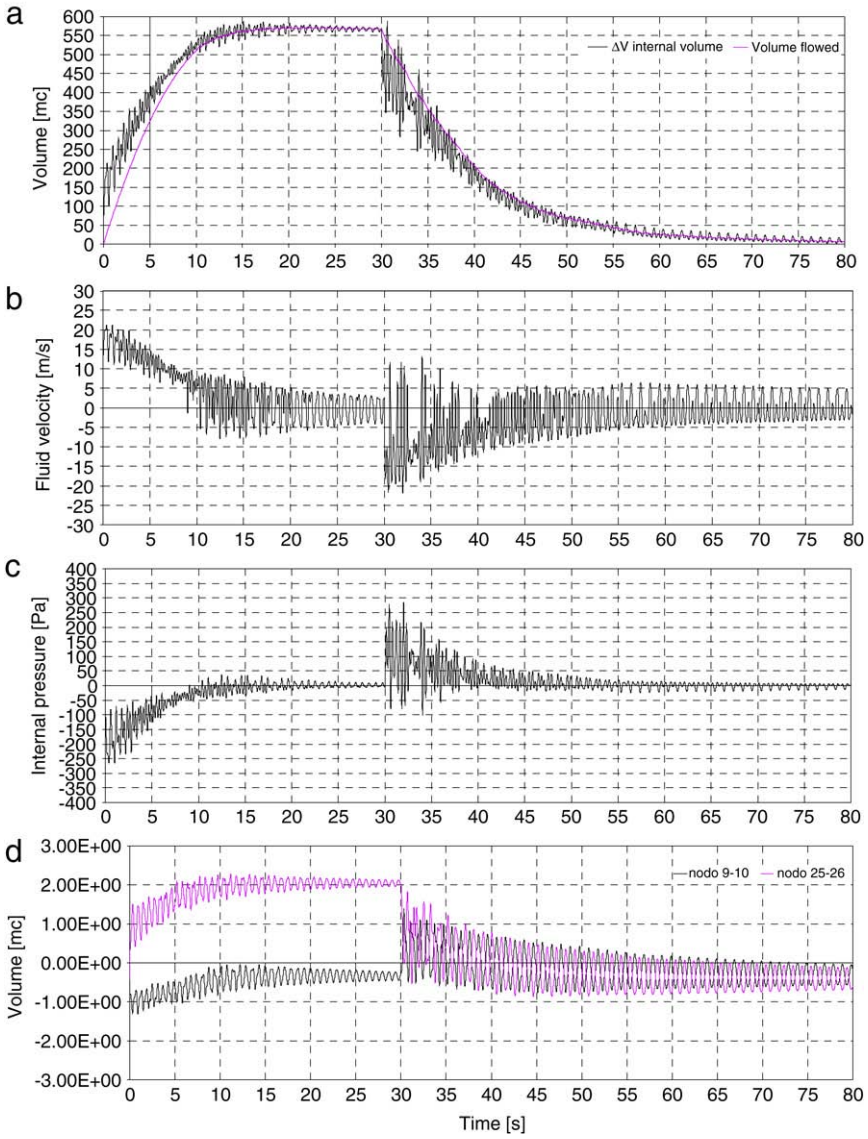

Fig. 14. 'Two Strips' — I° Phase: suction 1–30 s — II° Phase: free vibration 30–80 s. (a) Internal volume variation, (b) fluid velocity, (c) internal pressure and (d) exchange volume.

meaning of the evolution in time. Actual evolution at the local and transitory level is not adequately described by the previous proposed model, but it must be acknowledged that it enabled assessing the substantially increased structural model stiffness introduced by fluid internal volume participation in external force structural response. The contribution of a "volume spring" thus adds to classical structural stiffness, schematised as an average value applied as follower body-attached load.

The change of the response of such a volume could be taken account of during the analyses, since its variations due to possible exchange with the outside were computed.

One of the most interesting aspects of such an approach is thus identified in increased structural system response frequency if compared with a conventional analytical approach. The structure proved more sensitive to higher frequency force components and so higher frequency structural modes become more important.

The contribution of the internal volume to the overall final response can be identified by setting fluid exchange surfaces with the outside to different increasing values.

As the exchange surface increases, the internal volume contributes to the global response of the roof structure, only concerning higher frequency external load components. While for the lower frequency external load components, the structure does not show the effects of the internal volume constraint.

In essence, this constraint is a non-linear component of overall system stiffness, whose contribution is modulated by imposing a different value on the external fluid environment exchange surface.

5.3. Montreal roof analysis

Dynamic analyses are based on the combination of two transitory: during the first one the structure has been subjected to a linear load of 2.0 s duration, with intensity due to the mean wind velocity, while the second transitory deals with the study of the structural response due to pressure fluctuation (e.g. [5,12]). The wind load field is obtained by simulation of the wind velocity and pressure coefficients measured by wind tunnel tests.

The speed field was simulated at a 60° angle of incidence between average wind direction and main structure axis, this being the wind angle that had led to the membrane roof failure.

Dynamic analyses on the structure were performed with three different boundary conditions in terms of exchange surface between internal and external volume, and the wind applied was the same for all the following analyses:

Please cite this article in press as: Lazzari M, et al. Nonlinear F.E. analysis of Montreal Olympic Stadium roof under natural loading conditions. Engineering Structures (2008), doi:10.1016/j.engstruct.2008.07.010

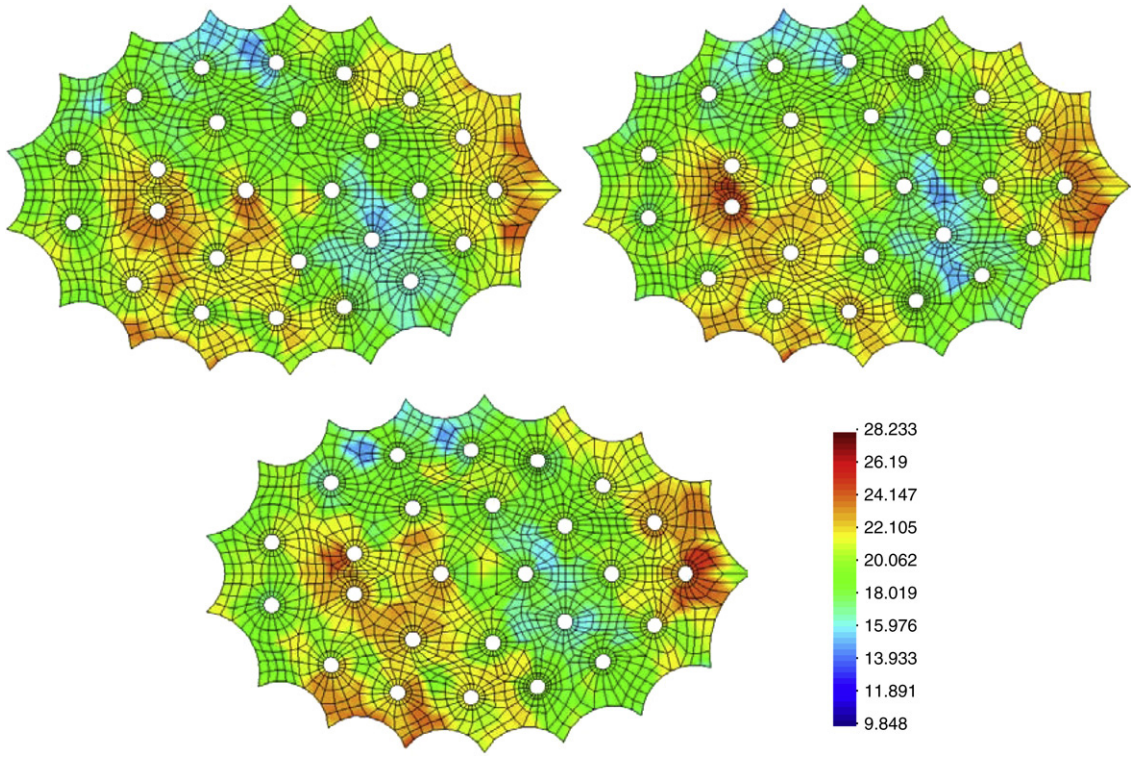

Fig. 15. Simulated wind velocity [m/s] at $2\Delta t = 0.4$ s in three subsequent instants.

- *analysis* I: *exchange surface* ∞, *no fluid structure interaction effect;*
- *analysis* II: 100 m^2 *exchange surface, permeable structure;*
- *analysis* III: 50 m^2 *exchange surface, permeable structure.*

An isothermal condition has been assumed, with a value of temperature of T = 298.15 °K (25 °C): such a value has been chosen to reproduce the environmental conditions for which the failure of the roofing system occurred.

The basic parameters for describing the wind generation model are [3,13–15] roughness Z_0=0.2 m, reference speed $V_{\text{ref}} = 17$ m/s at 10 m height and:

- *variation of wind speed with the height*:

$$\bar{V}(Z) = 2,5\, u^* \ln\left(\frac{Z}{Z_0}\right)$$

- *spectrum of longitudinal wind speed (PSD)*:

$$S(Z_i, n) = \left(\frac{u^{*2}}{n}\right)\left(\frac{2,21\beta^{2.5} f}{\left(1+3,31\beta^{1.5} f\right)^{5/3}}\right);$$

$$\beta = 5.53 \quad \text{and} \quad f = \frac{nz}{\bar{V}(Z)}$$

- *cross-spectrum:*

$$S_{jk}(n) = \sqrt{S_{jj}(n)\, S_{ii}(n)}\,\text{Coh}_{jk}(\omega)\, e^{-\text{in}2\pi\vartheta_{ij}}.$$

- *Vickery's coherence function:*

$$\text{Coh}_{ij}(y_i, z_i; y_j, z_j; n) = \exp\left(-2n\frac{\sqrt{C_Y^2(y_i - y_j)^2 + C_Z^2(z_i - z_j)^2}}{\bar{V}(z_k)}\right).$$

Wind induced load was generated by the simulation Shinozuka's algorithm developed by Deodatis, [16,17], considering: frequency field divisions $N_{\text{div}} = 2$, frequency interval splitting $N = 4096$, $\Delta t = 0.12$ s and generation steps 32768.

Model validation is reported in [14], while in Fig. 15 the velocity and its propagation above the structure in three subsequent instants are mapped. Vinckery's coherence for plane orthogonal to wind directions (cross-wind) with $C_Y = 11.5$; $C_Z = 11.5$ whereas the correlation of the signal in the own direction (along wind direction) is introduced by adding a delay in according with Taylor's hypothesis $\vartheta_{ij} = x_i/\bar{V}(z_i) - x_j/\bar{V}(z_j)$, i.e. Taylor's hypothesis states that the turbulence is converted downstream unchanged with the mean velocity (eg. [15,18]).

It is worth noting that the effect of using a quasi-static description for transforming wind velocity to pressure do not significantly affect the identification of the overall roof behaviour in terms of static and dynamic response. Nevertheless, a more refined modelling of fluid–structure interaction should be necessary to capture in detail the local behaviour of the structure characterised by a high flexibility that could changes the pressure field acting on the structure itself.

Moreover a comparison of the results obtained by numerical analyses of a large complex roof, composed by cables and membrane, with others analyses as well as with wind-tunneling tests, should be always carried out with care, since the hypotheses assumed as the basis of the results could be significantly different, and the final aim could be different as well. For these reasons, in the proposed research, some qualitative considerations, mainly concerning the global behavior of the analysed structure, have accompanied the necessary quantitative comparisons.

5.3.1. Results

The structure was analysed in time domain by using the classical Newmark algorithm, with γ parameter 0.5 and β parameter 0.25 and by using the iterative modified Newton–Raphson procedure. Such a Newmark algorithm, widely used to integrate the equations of evolution of dynamical systems, is proved to be unconditionally stable for linear problems, but only conditionally stable for non-linear problems (e.g. [19]). In particular the stability of

Please cite this article in press as: Lazzari M, et al. Nonlinear F.E. analysis of Montreal Olympic Stadium roof under natural loading conditions. Engineering Structures (2008), doi:10.1016/j.engstruct.2008.07.010

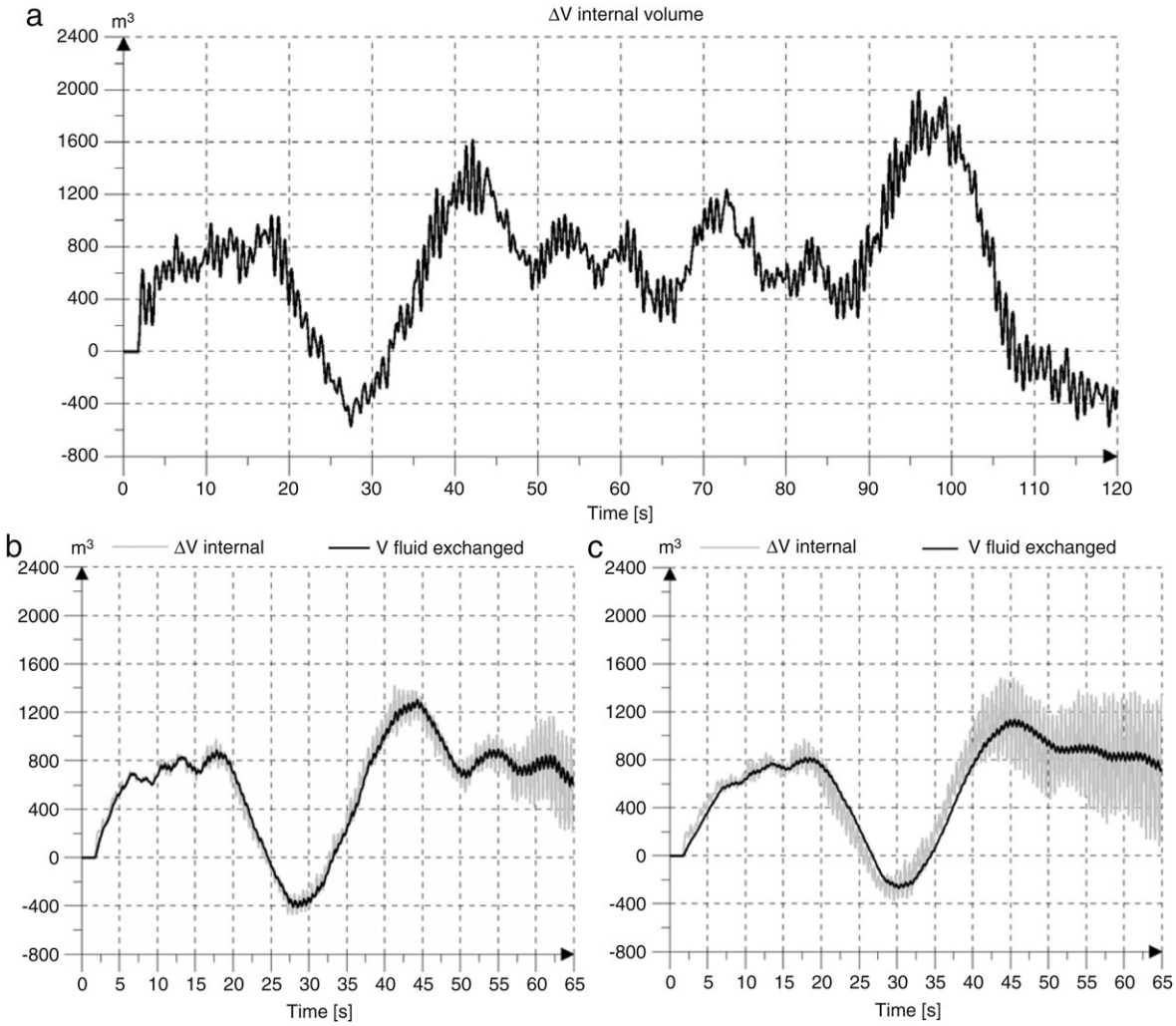

Fig. 16. Global parameter: Internal volume–exchange volume (a) ∞ m^2, (b) 100 m^2, (c) 50 m^2.

the Newmark algorithms in non-linear problems is related to the conservation of energy, and only for small time step sizes have they shown an excellent global energy behavior assuring stability condition.

In the proposed analyses, the presence of cables with small area and high stresses in the transition zone between suspension ropes and cone membranes, that is cables characterized by high frequency of vibration, affects and controls the time stepping size. The choice of $\Delta t = 0.04$ s assures avoiding any numerical instability risk: actually a numerical integration with a larger time step has shown to ill condition the solution, so producing a fast propagation of errors in successive time steps, mainly due to the artificial energy accumulation mechanism inside the structure.

Finally, a sufficiently small integration time step assures a better convergence in the presence of internal pressure compensation, due to the internal volume described in the previous sections.

The first analysis, with no fluid structure interaction effect, shows a response characterised by no aerodynamic resonance, so no risk factors are added to those already emphasised: Fig. 16a illustrates the diagram of the internal volume variation with time. Displacements and stresses remain limited (Fig. 17a), although complete unloaded appears in some cables, thereby representing a sudden tension recovery problem. The time series of displacement and stress indicate different signal frequency content at different membrane points.

The other two analyses, dealing with permeable structures (Fig. 16b and c), indicate the onset of aerodynamic resonance that increases as external exchange surface decreases, that is to say as the structure becomes more stiff and dissipates less energy due to decreased fluid volume pushed out or re-called by internal volume.

Internal pressure that usually never exceeds ± 9 Pa, varies within a range of ± 33 Pa during the resonance phenomenon, due to the internal volume ranging from 1200 m^3 to 1400 m^3 in less than 0.2 s. This volume oscillation develops at a very high frequency in airtight internal volume conditions. The displacement and stress time series for an almost central membrane point (Fig. 17b, c) clearly show the effect of dynamic resonance and how, in some cases, it occurs with non-linear pounding both for displacement and stress.

Concerning the suspension cables, as the dynamic analysis evolves, the structure changes its stiffness characteristic and in a number of cables tension zeroing occurs, mainly due to a significant variation in the displacement at cable ends. The variation of the vibration frequency is the effect of volume constraint induced by structural motion. As already specified, volume constraint leads to increased structural stiffness, and thus higher oscillation frequencies. These go away from the fundamental natural frequency, dependent on geometrical characteristics and stress state, approaching a higher frequency imposed on the cable during forced end motion.

Furthermore, suspension cables have a high structural mass and produce a great deal of kinetic energy due to large displacements. This can be ascribed to their length, sags and incapability to

Please cite this article in press as: Lazzari M, et al. Nonlinear F.E. analysis of Montreal Olympic Stadium roof under natural loading conditions. Engineering Structures (2008), doi:10.1016/j.engstruct.2008.07.010

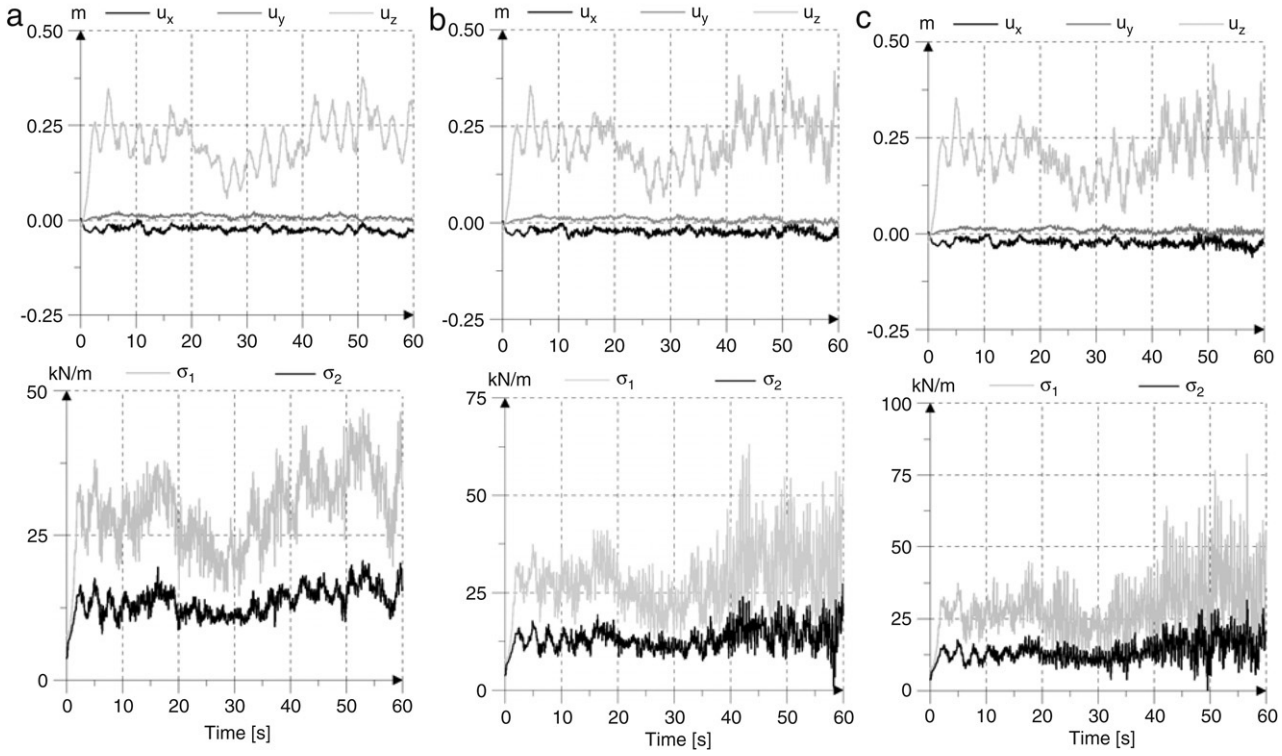

Fig. 17. Displacement [m] and stress [kN/m] node 745 (a) ∞ m^2, (b) 100 m^2, (c) 50 m^2.

effectively contrast structure motions by pre-tensioning induced into structure in the "state 0". The dynamic effect of cables is fundamental to correctly understand roof response, and particularly to explain the reasons and energy accumulation mechanisms underlying the failure that occurred in 1991, as can be gathered from eyewitnesses.

The kinetic energy developed by suspension cable motion leads to sudden dynamic-induced stress recovery. When coupled with large masses concentrated in the suspension cones, such recovery produces structural roof tearing. The study of the motion of some transversal roof sections (wind direction is 60°) shows two motion phases:

- 1st phase: the structure is characterised by not greatly correlated structural motions and the structural point displacements are essentially external load-dependent;
- 2nd resonance phase: the motions become quasi-antisymmetric and in this way the structure minimises the effects of internal pressure. Structural motion is dominated by the external pressure propagation and the constraint due to structural volume and motion of upper suspension cables.

The overall effect on the entire structure is a synchronisation of all the aspects that originate in time. This is matched with pressure wave propagation and leads to evident aerodynamic resonance.

6. Conclusions

The structural response of wide-span roofing such as the structure over the Montreal Stadium is particularly difficult to assess, essentially because of the geometrically non-linear behaviour this type of structure typically features and complexity of any bearing load simulation.

Analysis of the roof stress–load and displacement–load diagrams shows that structure behaviour is markedly non-linear. Large displacements under various load conditions lead to significant variations to roof structural stiffness and tensional state zeroing. Moreover the Montreal Stadium roof shows low structural stiffness and consequent excess deformability.

Any study performed in linear hypothesis is consequently not significant, and has slight relevance on real roof behaviour. Simulating static and dynamic loads requires using follower forces to follow up significant displacements. Tensional state zeroing and local instability further complicate solving the problem and require using highly specialised software.

Studies here carried out, enable identifying and better understanding its structural behaviour, emphasising the problems of the two cases considered and the potential solutions.

The aim of the proposed non linear dynamic analyses was to contribute to a better understanding of the local failure occurred for a wind load value less than the usual value assumed for the design of these structures.

References

[1] Melchers RE. Structural reliability. Elley Horwood Ltd; 1987.
[2] Majowiecki M. Snow and wind experimental analysis in the design of long-span sub-horizontal structures. J Wind Eng Ind Aerodyn 1998;74–76:795–807.
[3] Lazzari M, Saetta A, Vitaliani R. Non-linear dynamic analysis of cable-suspended structures subjected to wind actions. J Comput Struct 2001;79(9):953–69.
[4] Lazzari M, Vitaliani RV, Majowiecki M, Saetta AV. Dynamic behaviour of a tensegrity system subjected to follower wind loading. Comput Struct 2003;81(22–23):2199–217.
[5] Lazzari M. Geometrically non-linear structures subjected to wind actions. Ph.D. thesis. Italy: University of Padua; 2002.
[6] Kato S, Yoshino T, Minami H. Formulation of constitutive equations for fabric membranes based on the concept of fabric lattice model. Eng Struct 1999;21:691–708.
[7] Rossi R, Lazzari M, Vitaliani R, Oñate E. Simulation of light-weight membrane structures by wrinkling model. Int J Numer Methods Eng 2005;62(15):2127–53.
[8] Schweizerhof K, Ramm E. Displacement dependent pressure loads in nonlinear finite element analyses. Comput Struct 1984;18(6):1099–114.

Please cite this article in press as: Lazzari M, et al. Nonlinear F.E. analysis of Montreal Olympic Stadium roof under natural loading conditions. Engineering Structures (2008), doi:10.1016/j.engstruct.2008.07.010

[9] Schweizerhof K, Ramm E. Follower force effects on stability of shells under hydrostatic loads. J Eng Mech 1987;113(1):72–88.
[10] Bathe K-J. Finite element procedures in engineering analysis. Englewood Cliffs, New Jersey: Prentice-Hall Inc; 1996.
[11] Vitaliani RV, Gasparini AM, Saetta AV. Finite element solution of the stability problem for nonlinear undamped and damped systems under nonconservative loading. Int J Solids Struct 1997;34(19):2497–516.
[12] Borri C, Zahlten W. Fully simulated non linear analysis of large structures subjected to turbulent artificial wind. Mech Struct Mach 1991;19(2):213–50.
[13] Simiu E, Scanlan R. An introduction to wind engineering. John Wiley & Sons; 1996.
[14] Rossi R, Lazzari M, Vitaliani R. Wind field simulation for structural engineering purposes. Int J Numer Methods Eng 2004;61(5):738–63.
[15] Lazzari M, Majowiecki M, Saetta A, Vitaliani. Generazione artificiale dell'azione del vento: Analisi comparativa degli algoritmi di simulazione nel dominio del tempo, 5° Convegno Nazionale di Ingegneria del Vento. ANIV IN-VENTO-98; 1998 [in Italian].
[16] Shinozuka M, Jan CM. Digital simulation of random processes. J Sound Vib 1972;25:111–28.
[17] Deodatis G. Simulation of ergodic multivariate stochastic processes. J Eng Mech 1996;122:778–87.
[18] Scruton C. An introduction to wind effects on structures. Oxford University Press; 1990.
[19] Simo JC, Tarnow N, Wong KK. Exact energy—momentum conserving algorithms and symplectic schemes for nonlinear dynamics. Comput Methods Appl Mech Eng 1992;100(1)):63–116.

Please cite this article in press as: Lazzari M, et al. Nonlinear F.E. analysis of Montreal Olympic Stadium roof under natural loading conditions. Engineering Structures (2008), doi:10.1016/j.engstruct.2008.07.010